J Solid State Electrochem (1999) 3: 380–386

ORIGINAL PAPER

Magdy A.M. Ibrahim · Hamdy H. Hassan
Sayed S. Abd El Rehim · Mohamed A. Amin

The electrochemical behaviour of polycrystalline silver electrodes in Na_2CO_3 solution and the effect of ClO_4^- ions

Received: 3 July 1998 / Accepted: 10 March 1999

Abstract The electrochemical behaviour of polycrystalline silver electrodes in Na_2CO_3 solutions was studied under potentiodynamic and potentiostatic conditions and complemented with X-ray diffraction analysis. Potentiodynamic E/i anodic curves exhibit active passive transition prior to an oxygen evolution reaction. The active region involves a small peak AI followed by a major peak AII before the passive region. Peak AI is assigned to the formation of an Ag_2O layer while peak AII is due to the formation of an Ag_2CO_3 layer. The height of the anodic peaks increases with increasing Na_2CO_3 concentration, scan rate and temperature. The effect of increasing additions of $NaClO_4$ on the electrochemical behaviour of Ag in Na_2CO_3 solutions was investigated. The perchlorate ions stimulate the active dissolution of Ag, presumably as a result of the formation of soluble $AgClO_4$ salt. In the passive region, ClO_4^- ions tend to break down the dual passive film, leading to pitting corrosion at a certain critical pitting potential. The pitting potential decreases with ClO_4^- concentration. Potentiostatic current/time transients showed that the formation of Ag_2O and Ag_2CO_3 layers involves a nucleation and growth mechanism under diffusion control. However, in the presence of ClO_4^- ions, the incubation time for pit initiation decreases on increasing the anodic potential step.

Key words Silver electrode · Sodium carbonate · Sodium perchlorate · Pitting corrosion

Introduction

The electrochemical behaviour of silver in NaOH and KOH solutions has been intensively studied and numerous publications deal with the subject [1–8]. There exists a general agreement that the early stage of anodic oxidation in these alkaline solutions involves the formation of an Ag_2O layer through a nucleation and growth mechanism. Surprisingly, very little is known, however, about the electrochemistry of silver in carbonate solutions. Therefore, we felt that it is interesting to study the electrochemical behaviour of this system.

In the present work, the electrochemical behaviour of a polycrystalline silver electrode in sodium carbonate deaerated aqueous solutions has been studied. Various electrochemical techniques were used. Further experiments involving the effect of the presence of perchlorate ions (as aggressive ions) in carbonate solution were also carried out. The electrode surface was examined by X-ray diffraction (XRD).

Experimental

The measurements were performed in a conventional three-electrode electrolytic cell. The working electrodes were made of polycrystalline silver (99.99%, Koch Light, UK) rods axially embedded in Araldite holders to offer a circular silver exposed apparent area of 0.126 cm^2. The electrodes were mechanically polished starting with fine grained emery paper and followed with alumina paste to obtain a mirror-polished silver electrode surface, then rinsed with acetone and doubly distilled water. The counter electrode was a platinum wire. A saturated calomel electrode (SCE) connected to the cell by a bridge with a Luggin-Haber capillary tip served as the reference electrode for all potentials quoted in this paper.

Measurements were performed in Na_2CO_3 solutions without and with the addition of $NaClO_4$. All solutions were freshly prepared from analytical grade reagents and doubly distilled water. Each solution was deaerated by bubbling N_2 prior to taking any measurements and was purged continuously throughout the experiment. All runs were conducted at a constant temperature ± 0.5 °C.

Potentiodynamic measurements were carried out using a potentioscan type (Potentiostat-Galvanostat model 273 EG&G) connected to an X-Y recorder (series 2000 Omingraphic).

Potentiostatic current/time transients at constant potentials E_s were carried out as follows: the electrode was held at $E = -2000$ mV for 60 s to obtain a reproducible electroreduced silver surface, then immediately stepped to an anodic E_s at which the current transient was recorded as a function of time.

M.A.M. Ibrahim (✉) · H.H. Hassan
S.S. Abd El Rehim · M.A. Amin
Chemistry Department, Faculty of Science,
Ain Shams University, Abbassia, Cairo, Egypt
e-mail: imagdy@asunet.shams.eun.eg

The composition of the passive film formed on the silver anode was examined by XRD analysis using a Philips P.W. Model 1730 diffractometer with Cu-K_α radiation and an Ni filter. It was adopted at 40 kV and 25 mA.

Results and discussion

Potentiodynamic polarization measurements

Figure 1 illustrates the potentiodynamic E/i anodic curves for polycrystalline Ag in quiescent Na_2CO_3 solutions of various concentrations (0.25–1.5 M) recorded between −2000 and 1250 mV (SCE) with a scan rate (v) of 100 mV s^{-1} and at 25 °C. The anodic responses are characterized by the occurrence of an active/passive transition state prior to an oxygen evolution reaction. The active region involves two anodic peaks, a small peak (AI) and a major peak (AII) prior to the passive region.

Visual inspection of the electrode showed that when it was potentiodynamically polarized to the oxygen evolution reaction, a thick grey film was observed on its surface. It seems that this layer is not highly protective since the passivation current (i_{pass}) is not very small (about 6 mA in 0.5 M Na_2CO_3). XRD analysis showed that the passive film formed within the range of peak AI consisted of Ag_2O (Fig. 2a), while the deposit found on the surface in the range of peak AII consisted of Ag_2O and Ag_2CO_3 (Fig. 2b). Therefore, according to XRD data and by comparing the measured potentials with the equilibrium potentials for the most probable electrooxidation reactions for Ag in aqueous Na_2CO_3 solution, one can conclude that the anodic peaks AI and AII may be ascribed to successive establishment of the systems Ag/Ag_2O and Ag/Ag_2CO_3 respectively on the electrode surface [9], according to the overall reactions:

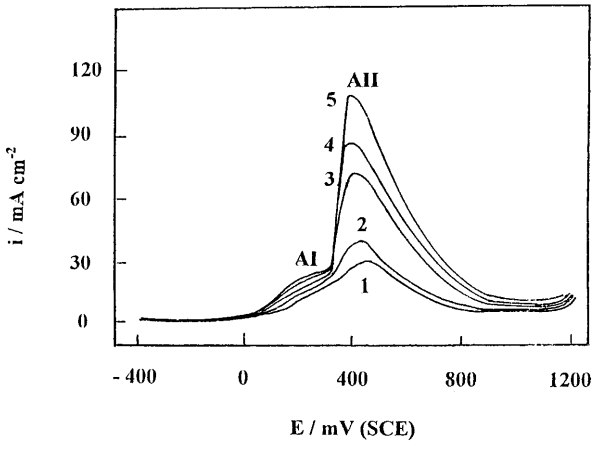

Fig. 1 Potentiodynamic polarization curves for a polycrystalline Ag anode in various concentrations of Na_2CO_3 at 25 °C and a scan rate of 100 mV s^{-1}: (*1*) 0.25 M, (*2*) 0.50 M, (*3*) 0.75 M, (*4*) 1.0 M, (*5*) 1.5 M Na_2CO_3

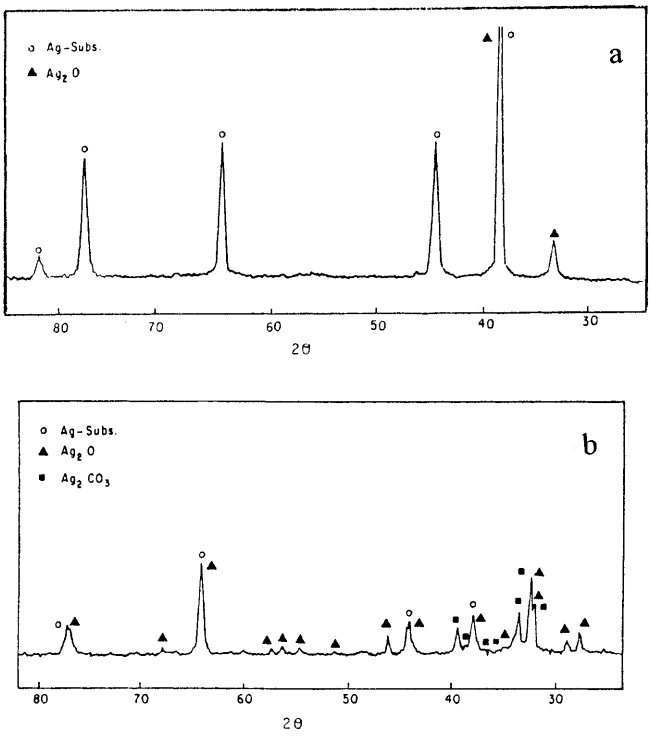

Fig. 2 X-ray diffraction pattern for an Ag anode in 0.5 M Na_2CO_3 at a scan rate of 100 mV s^{-1} potentiodynamically polarized: within the potential range of peak A1 (**a**) and within the potential range of peak AII (**b**)

$$2Ag + 2\ OH^- \rightarrow Ag_2O + H_2O + 2e^- \quad E^\circ = 344\ mV \tag{1}$$

$$2Ag + CO_3^{2-} \rightarrow Ag_2CO_3 + 2e^- \quad E^\circ = 477\ mV \tag{2}$$

The OH^- ions are preferentially adsorbed on the active sites of the metal surface since their polarizabilities are greater than those of CO_3^{2-} ions [9]. The preferable adsorption of OH^- ions assists the formation of an Ag_2O thin solid phase on the surface (peak AI). Likewise, when the applied potential exceeds that of peak AI, the depletion of OH^- ion concentration at the electrode surface allows the formation of an Ag_2CO_3 salt layer (peak AII) on top of the inner Ag_2O film. These results indicate that the presence of an Ag_2O film on the surface does not preclude the formation of Ag_2CO_3.

Inspection of the results of Fig. 1 reveals also that the height of peaks AI and AII increases, and their corresponding peak potentials shift towards more negative values, with increasing carbonate concentration. The passivity current i_{pass} also increases with the electrolyte concentration. The linear dependence of peak current densities (i_{PAI}) and (i_{PAII}) on carbonate concentration ($C_{CO_3^{2-}}$) in semilogarithmic coordinate form is shown in Fig. 3. This behaviour may be explained in terms of the increasing solubilities of Ag_2O and Ag_2CO_3 with increasing pH [10].

The effect of the potential scan rate v (10–400 mV s^{-1}) on the polarization responses for Ag in 0.5 M Na_2CO_3 at

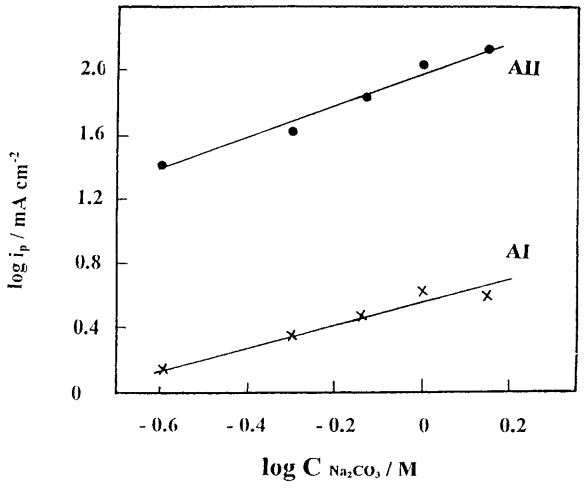

Fig. 3 Dependence of the peak current density i_p of the two anodic peaks AI and AII on the concentration of Na_2CO_3; quiescent solutions (data taken from Fig. 1)

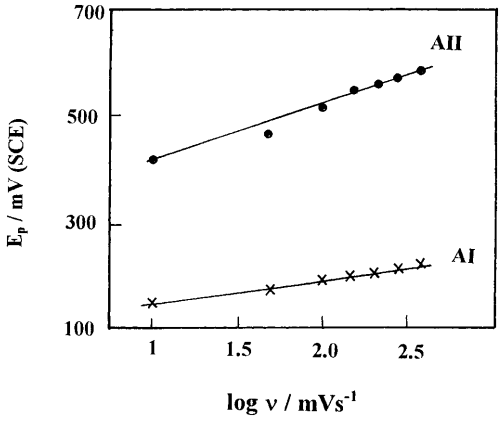

Fig. 5 Dependence of the peak potential E_p of the two anodic peaks AI and AII on the logarithm of the scan rate for polycrystalline Ag in 0.5 M Na_2CO_3

25 °C was determined. The results reveal that the peak current densities i_{PAI} and i_{PAII} of the two anodic peaks increase and their corresponding potentials E_{PAI} and E_{PAII} shift to more positive potentials with increasing v. The dependence of i_{PAI} and i_{PAII} on $v^{1/2}$ is given in Fig. 4, where straight lines passing through the origin are obtained; the slopes of the two lines are 0.63 and 5.10, respectively. Moreover, Fig. 5 shows a satisfactory linear fit with E_{PAI} and E_{PAII} versus log v; the slopes of the two lines are 55.0 and 91.2 s, respectively. These data suggest that the formation of Ag_2O and Ag_2CO_3 solid films is mainly controlled by the diffusion of the reacting species, as well demonstrated in the analyses of Randles [11] and Sevick [12].

The influence of temperature (15–70 °C) on the potentiodynamic anodic responses for Ag in quiescent 0.5 M Na_2CO_3 and at $v = 100$ mV s^{-1} was investigated. The data (not included) demonstrate that the rise of temperature enhances the height of the peak current densities of the two anodic peaks and shifts their peak potentials to more negative values.

The effect of the addition of $NaClO_4$ to Na_2CO_3 solutions on the electrochemical behaviour of Ag was investigated. Figure 6 shows some examples of the effect of adding increasing amounts (0.07–0.70 M) of $NaClO_4$ to 0.5 M Na_2CO_3 at 25 °C and 10 mV s^{-1}. The data reveal that the presence of ClO_4^- ions results in an increase of the peak currents of peak AI and peak AII proportional to the ClO_4^- concentration. The relation between i_{PI} and i_{PII} versus log $C_{ClO_4^-}$ is given in Fig. 7. Such an influence of ClO_4^- on the anodic dissolution of Ag through peaks AI and AII can be related to the high specific adsorbability of ClO_4^- ions on the energetically preferred sites on the Ag surface [13, 14] in competition with OH^- and CO_3^{2-} ions, whose adsorption is essential for the formation of Ag_2O and Ag_2CO_3, respectively.

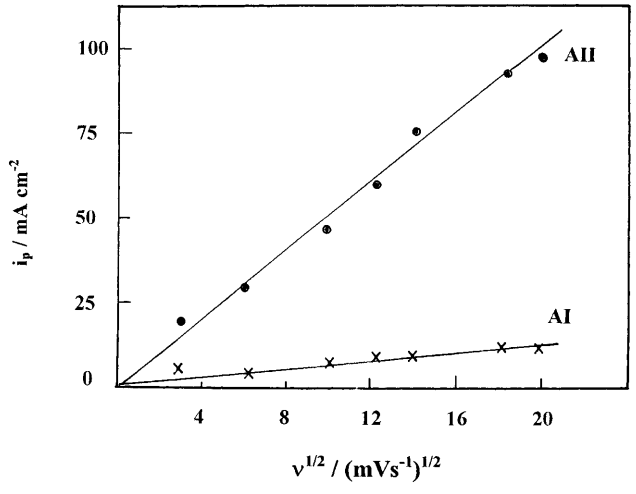

Fig. 4 Dependence of the peak current density i_p of the two peaks AI and AII on the square root of the scan rate for a polycrystalline Ag anode in 0.5 M Na_2CO_3 at 25 °C

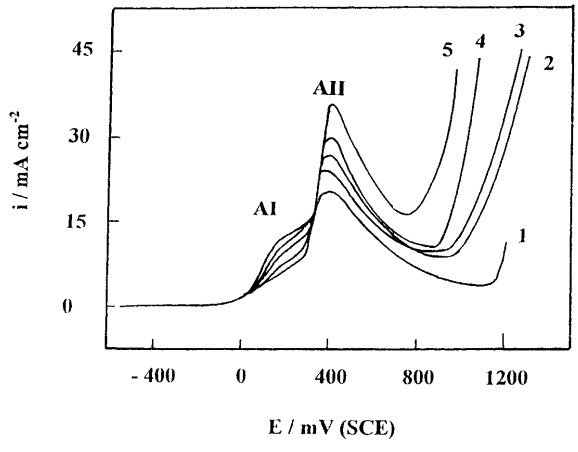

Fig. 6 Influence of $NaClO_4$ concentration added to 0.5 M Na_2CO_3 on the potentiodynamic polarization curves for a polycrystalline Ag anode, at 25 °C and a scan rate of 10 mV s^{-1}: (*1*) 0.0, (*2*) 0.07, (*3*) 0.1, (*4*) 0.5, (*5*) 0.7 M $NaClO_4$

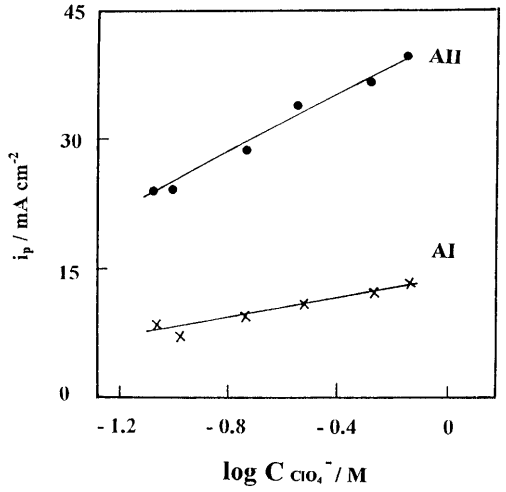

Fig. 7 Dependence of the peak current density i_p of the two peaks on the $NaClO_4$ concentration added to 0.5 M Na_2CO_3 for a polycrystalline Ag anode at 25 °C and a scan rate of 10 mV s^{-1}

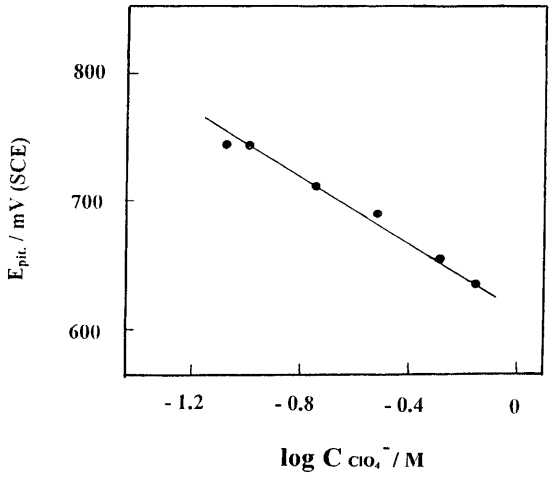

Fig. 8 Dependence of pitting potential E_{pit} on the $NaClO_4$ concentration added to 0.5 M Na_2CO_3 for a polycrystalline Ag anode at 25 °C and a scan rate of 10 mV s^{-1}

The adsorbed ClO_4^- ions might participate directly in anodic dissolution and formation of soluble $AgClO_4$ salt according to the reaction:

$$Ag + ClO_4^- \rightarrow AgClO_4 + e^- \quad (3)$$

Therefore, one can conclude that each anodic current peak is indicative of two processes: the dissolution of metal and the formation of soluble $AgClO_4$ salt and the precipitation of Ag_2O film (peak AI) and Ag_2CO_3 (peak AII).

On the other hand, the presence of ClO_4^- ions in the carbonate solution causes drastic changes in the passive region where the passive current density i_{pass} is enhanced in the presence of ClO_4^- ions, and at a certain critical potential, E_{pit}, it rises suddenly, without any sign of oxygen evolution, indicating breakdown of the dual passive layer and initiation and growth of pitting corrosion. The aggressive action of ClO_4^- addition towards the stability of the passive film may be due to its ability to adsorb on the passivated surface. Above a certain specific concentration, the adsorbed ClO_4^- anions become incorporated in, and penetrate, the passive film under the influence of an electric field across the film solution interface [15]. When the field reaches a certain value corresponding to E_{pit}, the aggressive anions break down the dual film. Once a pit is nucleated, pitting growth is believed to proceed in the active dissolution mode. Pit growth occurs as a result of an increase in the perchlorate ion concentration, resulting from its migration inside pits. It is clear that an increase in ClO_4^- ion concentration shifts E_{pit} towards a more negative (active) direction. Plots of E_{pit} versus log $C_{ClO_4^-}$ give a straight line (Fig. 8) according to the equation:

$$E_{pit} = a - b \log C \quad (4)$$

where a and b are constants. This relation is analogous to the phenomena that are commonly recognized in studies of pitting corrosion on some metals by the presence of aggressive anions [16–19].

Stepwise cyclic voltammetric measurements

Figure 9 shows an example of cyclic voltammograms started from −1800 mV and reversed at various anodic potential steps (E_s) with the same scan rate (v = 10 mV s^{-1}) in 0.5 M Na_2CO_3 at 25 °C. It is found that if

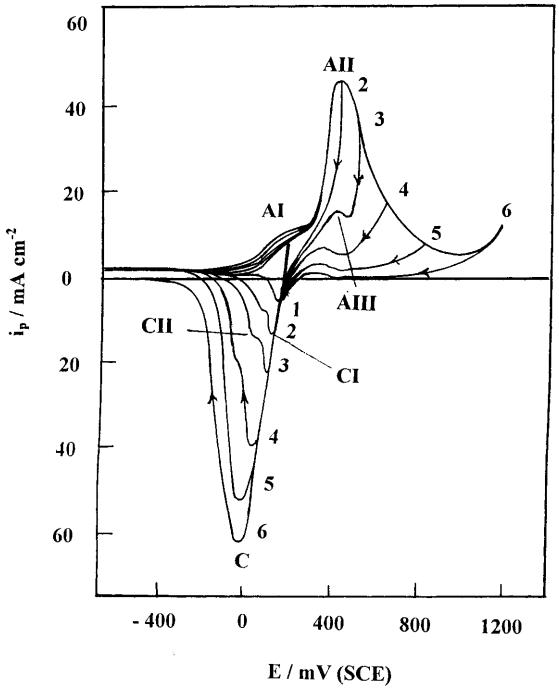

Fig. 9 Cyclic voltammograms for a polycrystalline Ag electrode in 0.5 M Na_2CO_3 at 25 °C starting from −1800 mV and reversed at various anodic potentials (scan rate 10 mV s^{-1})

the anodic potential steps are reversed within the potential region of peak AI, the cathodic scan exhibits one cathodic peak (CI); therefore peak CI is assigned to the reduction of Ag_2O to Ag. However, when E_s is extended into the potential range more positive than that of peak AI, the reverse scan exhibits a reactivation anodic peak (AIII) in addition to a second cathodic peak (CII) which appears at first as a hump on the negative side of peak CI. Peak CII is assigned to the reduction of Ag_2CO_3 to Ag. It is seen that the contribution of peaks CI and CII increases when E_s is made more positive. Finally, peak CII surpasses the area of peak CI and the two peaks appear as a single compound peak C (CI/CII). The appearance of peak AIII is symptomatic of a reactivation process, whereby the passive layers are practically dissolved by the electrolyte at weak and defect points. Such activated points allow the electrodissolution of the metal and formation of Ag^+ ions.

Figure 10 presents some cyclic voltammograms for Ag in 0.5 M Na_2CO_3 containing 0.5 M $NaClO_4$ obtained with a progressively varied anodic potential step. For $E_s < E_{pit}$, i.e. in absence of pitting, the shape of these voltammograms is similar to those given in Fig. 9: at first the two peaks CI and CII appear and then the compound peak C appears instead of these two cathodic peaks, with increasing values of E_s. For $E_s > E_{pit}$, i.e. in the presence of pitting, the pitting current density i_{pit} shows slight hysteresis between the forward and reverse scans and decreases rapidly, reaching a zero value at a certain potential (repassivation) without the appearance of the activated peak AIII. The cathodic excursions show two cathodic peaks, the compound peak C and a new peak CIII. The latter peak can be related to the reduction of the soluble pitting corrosion products. The contribution of peaks C and CIII increases with increasing the value of E_s.

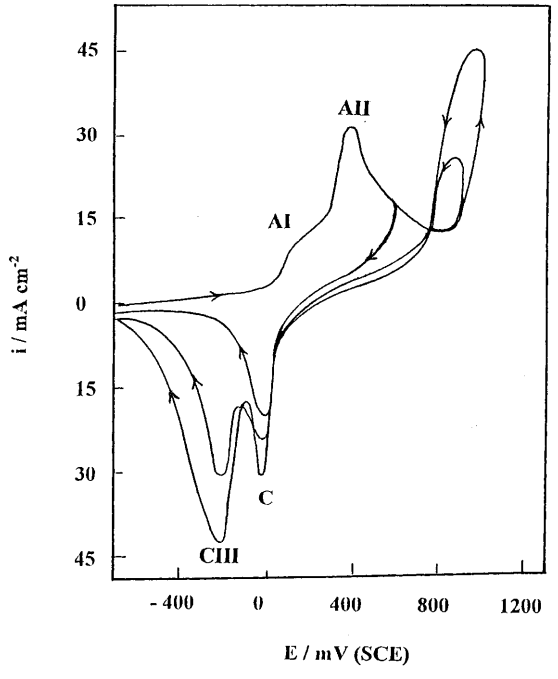

Fig. 10 Cyclic voltammograms for a polycrystalline Ag electrode in a solution containing 0.5 M Na_2CO_3 + 0.5 M $NaClO_4$ at 25 °C starting from −1800 mV and reversed at various anodic potentials (scan rate 10 mV s^{-1})

Current/time transients measurements

In order to gain more information about the electrochemical behaviour of Ag in Na_2CO_3 solutions in the absence and presence of $NaClO_4$, potentiostatic current/time transients were performed at various anodic steps E_s. Figure 11 shows the current transients for Ag in perchlorate-free 0.5 M Na_2CO_3 solution at 25 °C. It is seen that the current transient densities decrease monotonically with time to reach a steady state value. As the step potential is made more positive, the values of the instantaneous and steady state currents increase, indicating an increase in the thickness of the anodically formed layers. The continuously decreasing parts of the current transients fit linear i versus $t^{-1/2}$ relationships (Fig. 12), going through the origin, and show two interesting features. Firstly, for $E_s < 300$ mV there are single slopes as one would expect, owing to the formation of an Ag_2O layer. For $E_s > 300$ mV, a break in the plots is observed, each portion obeying a linear relationship. The data are consistent with the formation of two distinct anodic layers in different potential ranges. It is probable that the formation of these two passive layers involves a nucleation and growth mechanism under diffusion control.

Figure 13 shows an example of the current/time transients for Ag in 0.5 M Na_2CO_3 containing 0.1 M $NaClO_4$ recorded at various densities with time, similar to those observed in Fig. 11. For $E_s > E_{pit}$, the current

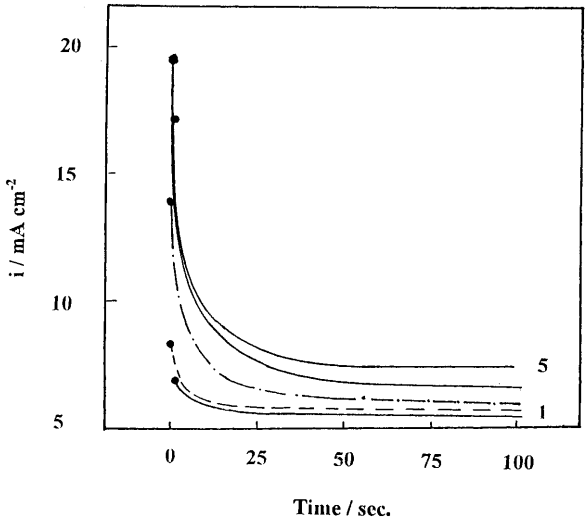

Fig. 11 Current transients vs. time recorded in 0.5 M Na_2CO_3 at 25 °C at constant anodic step potentials: (*1*) 100 mV, (*2*) 300 mV, (*3*) 400 mV, (*4*) 600 mV, (*5*) 900 mV

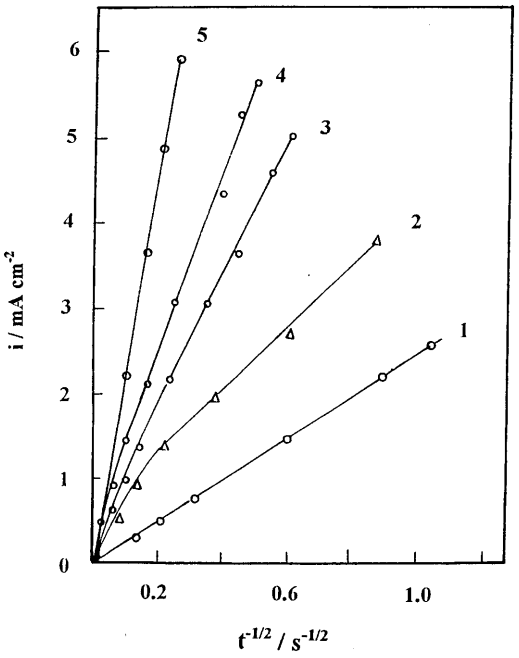

Fig. 12 Dependence of the current density on $t^{-1/2}$ for the descending portions of the current transients for a polycrystalline Ag electrode in 0.5 M Na_2CO_3 at 25 °C: (*1*) 100 mV, (*2*) 300 mV, (*3*) 400 mV, (*4*) 600 mV, (*5*) 900 mV

initially decreases to a minimum value i_{pass}, yielding the corresponding characteristic pitting time parameter, namely the incubation time t_i (the time needed for ClO_4^- ions to penetrate the dual passive layer and initiate pitting). As E_s is set more positive, the incubation period becomes shorter. After the incubation time, the current starts to rise steadily as a result of pit growth. Figure 14 shows that the growth current density i_{pit} associated with

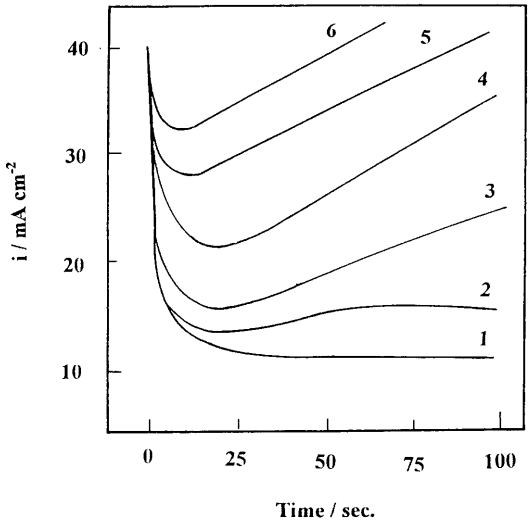

Fig. 13 Current transients vs. time recorded in a solution containing 0.5 M Na_2CO_3 + 0.1 M $NaClO_4$ at 25 °C at constant anodic step potentials: (*1*) 450 mV, (*2*) 500 mV, (*3*) 600 mV, (*4*) 650 mV, (*5*) 700 mV, (*6*) 750 mV

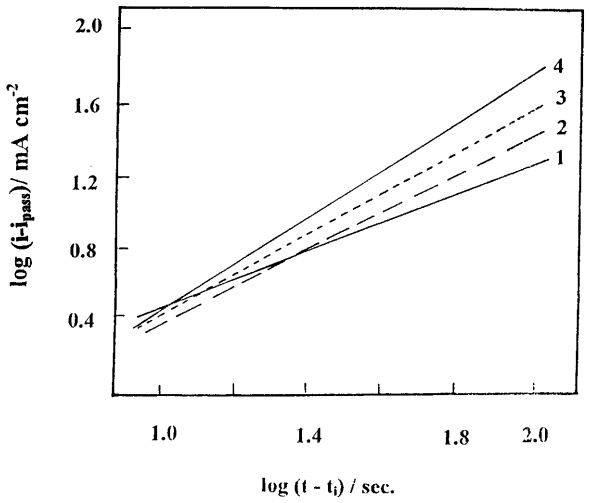

Fig. 14 Dependence of $\log(i-i_{pass})$ vs. $\log(t-t_i)$ for a polycrystalline Ag electrode in 0.5 M Na_2CO_3 + 0.1 M $NaClO_4$ at different anodic step potentials: (*1*) 600 mV, (*2*) 650 mV, (*3*) 700, (*4*) 750 mV

pit growth varies linearly with time and fits the Engell-Stolica equation for pitting corrosion [20]:

$$i_{pit} = \left(i - i_{pass}\right) = k(t - t_i)^b \quad (5)$$

where i is the current density measured on the whole specimen area, i_{pass} is the passivity current, t_i is the incubation time and k and b are constants. The values of k and b are given in Table 1. The results indicate that the values of k and b depend on the anodic step potential. The pit growth current density i_{pit} enhances on increasing the anodic potential step E_s. Such behaviour suggests that there is a distribution of the nucleation sites of different energies which nucleate at distinct potentials [21] or, in other words, the more positive is E_s, the more will be the activated sites.

Conclusions

- The electrochemical behaviour of a polycrystalline silver electrode in sodium carbonate solution free from and containing sodium perchlorate was examined using potentiodynamic and potentiostatic techniques.
- In perchlorate-free carbonate solutions the anodic polarization curves show active/passive transition states. The active region exhibits two anodic peaks, a

Table 1 The values of the constants k and b in Eq. (5)

E_s (mV)	k	b (mA cm^{-2} s^{-1})
600	2.1	0.75
650	1.6	0.99
700	1.7	1.10
750	1.7	1.25

small peak AI followed by a major peak AII, their appearance related to the formation of Ag_2O and Ag_2CO_3 layers, respectively. The formation of these two layers involves a nucleation and growth mechanism under diffusion control.

- The passive film is dual in nature, consisting of an inner Ag_2O layer and an outer Ag_2CO_3 layer.
- The anodic dissolution of a silver electrode through the active and passive regions increases with increasing carbonate concentration, scan rate and temperature.
- The cathodic polarization curve shows two cathodic peaks, CI (conjugates to peak AI) and the more negative CII (conjugates to peak AII). The two cathodic peaks tend to coalesce with each other and appear as one compound peak C on increasing the anodic potential.
- The addition of ClO_4^- ions to the carbonate solution stimulates the active dissolution of the silver anode and tends to break down the dual passive film and initiate a pitting attack at a certain critical pitting potential. The pitting potential shifts towards a more negative (active) direction with increasing ClO_4^- ion concentration.
- The potentiostatic examination revealed that the incubation time (the time required for ClO_4^- ions to penetrate the passive layer and initiate pitting corrosion) decreases and the pit growth current increases on increasing the anodic potential step.

References

1. Tilak BV, Perkins RS, Kozlowska HA, Conway BE (1972) Electrochim Acta 17: 1447
2. Sato N, Shamizu Y (1973) Electrochim Acta 18: 567
3. Hepel M, Tomkiewicz M (1984) J Electrochem Soc 131: 1288
4. Hepel M, Tomkiewicz M, Forest CL (1986) J Electrochem Soc 133: 468
5. Gomez Becerra J, Salvarezza RC, Arvia AJ (1988) Electrochim Acta 33: 1431
6. Salvarezza RC, Gomes Becerra J, Arvia AJ (1988) Electrochim Acta 33: 1753
7. Alonso C, Salvarezza RC, Vara JM, Arvia AJ (1990) Electrochim Acta 35: 489
8. Dirkse TP (1990) Electrochim Acta 35: 1445
9. Weart RC (1974) Handbook of chemistry and physics, 55th edn. CRC Press, Boca Raton
10. Druskovich DM, Ritchie IM, Singh P, Guang ZH (1989) Electrochim Acta 34: 409
11. Randles JB (1948) Trans Faraday Soc 44: 327
12. Sevick A (1948) Collect Czech Chem Commun 13: 349
13. Valette G (1982) J Electroanal Chem 138: 285
14. Valette G (1983) J Electroanal Chem 146: 439
15. Hoar TP, Mears D, Rothwell G (1965) Corros Sci 5: 279
16. Abd El Rehim SS, Taha F, Saleh MB, Mohamed SA (1992) Corros Sci 33: 1789
17. Abd El Rehim SS, El Basosi AA, Osman MM (1993) J Electroanal Chem 348: 99
18. Abd El Rehim SS, Fouad EE, Abd El Wahaab SM, Hassan HH (1996) J Electroanal Chem 401: 113
19. Refaey SAM, Abd El Rehim SS (1996) Electrochim Acta 42: 667
20 Engell HJ, Stolica DN (1959) Z Phys Chem Unterr 20: 133
21. Hills GJ, Shiffrin DJ, Thompson J (1974) Electrochim Acta 19: 657